Two-dimensional Thermal Modeling of Lithium-ion Battery Cell Based on Electrothermal Impedance Spectroscopy

Swierczynski, Maciej Jozef; Stroe, Daniel Loan; Knap, Vaclav; Kær, Søren Knudsen; Teodorescu, Remus

Published in:
ECS Transactions

DOI (link to publication from Publisher):
10.1149/07211.0033ecst

Publication date:
2016

Document Version
Accepted author manuscript, peer reviewed version

Two-dimensional Thermal Modeling of Lithium-ion Battery Cell Based on Electrothermal Impedance Spectroscopy

M. Swierczynski[a], D. I. Stroe[a], V. Knap[a], S. K. Knudsen[a], and R. Teodorescu[a]

[a] Department of Energy Technology, Aalborg University, Pontoppidanstræde 111, Denmark

Thermal modeling of lithium-ion batteries is gaining its importance together with increasing power density and compact design of the modern battery systems in order to assure battery safety and long lifetime. Thermal models of lithium-ion batteries are usually either expensive to develop and accurate or equivalent thermal circuit based with moderate accuracy and without spatial temperature distribution.

This work presents initial results that can be used as a fundament for the cost-efficient development of the two-dimensional thermal model of lithium-ion battery based on multipoint electrothermal impedance spectroscopy.

Introduction

Lithium-ion (li-ion) batteries are currently a first choice technology on the market of portable electronics and electro-mobility (EVs, HEVs, and PHEVs). Nevertheless, market standards and requirements for li-ion batteries are raising in order to meet demands of ever constantly growing demands of applications. Current research in li-ion batteries, amongst others, is aiming at increasing both energy and power densities of the modern li-ion batteries.

New battery applications may require high power charge and discharge rates in short to medium timescales (HEV, PHEVs). Thus, some li-ion battery chemistries, like $LiMO_2$/ $Li_4Ti_5O_{12}$ (*M* stands for metal) are capable of continuously delivering charge/discharge current rates of 10C and charge/discharge current pulses over 20C. This high power released in the nowadays space optimized battery packs may result in quick and significant temperature rise that may compromise safety (e.g. thermal runaways), battery performance. Moreover, electro-mobility applications are requiring 10-15 years of battery operation in the highly variable temperature environment that will be difficult to obtain without adequate information about battery cells heat generation and proper thermal management of battery packs. In consequence, the thermal modeling and estimation of battery temperature at different operating conditions is gaining its importance.

Battery thermal modeling

Widely used thermal modeling approaches are based on the finite element methods (FEMs) (1-4). The advantage of these models is their high accuracy and information about spatial battery temperature distribution. On the other hand, these thermal modeling approaches usually require a coupled electrochemical model and in consequence, computation burden is high and they cannot be executed in the real-time. Moreover, the parametrization of these models is complex and not time- and cost-efficient.

For less demanding applications, to overcome these difficulties, thermal models are simplified to the form of equivalent thermal circuits (ETC), where resistors, capacitors, and current sources are used for representing heat transfer, heat accumulation and heat source, respectively (5). ETC based models are a good compromise between the complexity and accuracy. Transition to these models is for the cost of losing spatial temperature resolution as these models are usually providing only information about average battery temperature. Although ETC based models are simpler in development, require expensive calorimeters or time consuming and destructive disassembling and the opening of battery cells in order to determine battery parameters like heat capacity, thermal conductivity and convective heat exchange with the environment. Thus, an alternative method, for parametrizing ETC based models, based on the electrothermal impedance spectroscopy (ETIS) was proposed in the literature (6-8).

In this work, initial results of the multipoint ETIS method for quick and cost-efficient ETC based model characterization is presented. The method can facilitate in the 2D and 3D ETC based thermal modeling of lithium-ion batteries without any a priori knowledge about li-ion battery cell's internal composition.

The principle of the electrothermal impedance spectroscopy

Although there are many different methodologies for the ETIS measurements on a battery cell that can be found in literature, in this work the focus was on 'frequency-based ETIS method' as it is the most accurate for determining heat capacity and heat conductivity of a battery cell (6).

The general concept of the ETIS is based on the similar principle as in the case of the Electrochemical Impedance Spectroscopy (EIS). In the case of the EIS, the electrical transfer function is determined by means of Laplace transformation in the frequency domain [1]. However, in the case of the ETIS, the thermal transfer function is being determined in the frequency domain based on the equation [2] (9).

$$Z_{TH} = \frac{U(j\omega_{EL} t)}{I(j\omega_{EL} t)} = \frac{\check{U} \cdot e^{j(\omega_{EL} t + \varphi_U)}}{\check{I} \cdot e^{j(\omega_{EL} t + \varphi_I)}} = \frac{\check{U}}{\check{I}} \cdot e^{(\varphi_U - \varphi_I)} \quad [1]$$

$$Z_{TH} = \frac{T(j\omega_{TH} t)}{Q(j\omega_{TH} t)} = \frac{\check{T} \cdot e^{j(\omega_{TH} t + \varphi_T)}}{\check{Q} \cdot e^{j(\omega_{TH} t + \varphi_Q)}} = \frac{\check{T}}{\check{Q}} \cdot e^{(\varphi_T - \varphi_Q)} \quad [2]$$

where: Z_{TH} is the thermal impedance, $T(j\omega_{TH}t)$ is the temperature response as function of time on the battery cell surface(amplitude $\check{T}$), $Q(j\omega_{TH}t)$ is the heat flow as function of time (amplitude $\check{Q}$), $j\omega_{TH}$ is equal to $j2\pi f_{TH}$, f_{TH} is the frequency of the heat excitation signal and φ_T, φ_Q are the phase angles of the temperature and heat flow, respectively.
The terms are analogously defined for the voltage (*U*) and current (*I*) of the electrical transfer function in equation [1].

In order to perform the frequency-based ETIS measurement, a low frequency sinusoidal shaped heat excitation signal is applied to the battery and battery surface sinusoidal temperature response is being measured (Figure 1). The entire process is being repeated for the series of frequencies and the thermal transfer function is obtained.

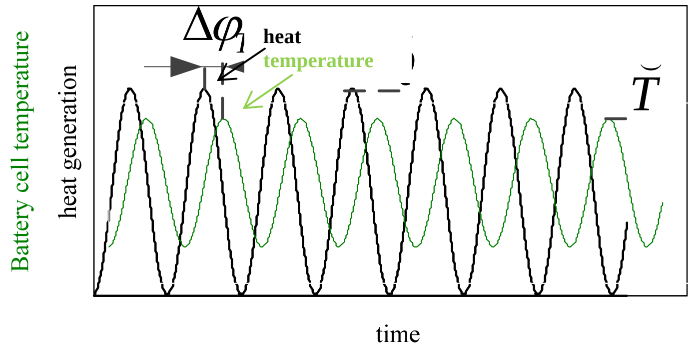

Figure 1. Illustration of the principle of the ETIS concept.

A detailed description of the method can be found in (6), (9).

Multipoint electrothermal impedance spectroscopy

So far, in the literature, the single point ETIS measurements were presented in the literature in order to determine battery cells' heat capacity and heat conductivity. These parameters were later used in the simple ETC based models in order to estimate an average temperature of battery cells. However, for some applications (e.g. battery pack design), it is beneficial to have more detailed information about spatial temperature distribution of battery cell in order to cool efficiently the hottest spots and avoid high-temperature gradients between different locations of the battery cell. This temperature difference was found to be even up to 9°C for the $LiMO_2/Li_4Ti_5O_{12}$ battery cell at during charging/discharging at high current rates (Figure 2).

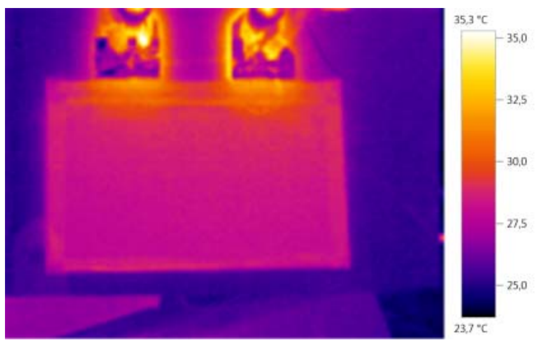

Figure 2. The non-uniform temperature of the $LiMO_2$/ $Li_4Ti_5O_{12}$ during charging.

TABLE I. Parameters of the high power lithium titanate oxide battery used for ETIS measurements.

Property	**$LiMO_2/Li_4Ti_5O_{12}$**
Nominal capacity	13 Ah
Nominal voltage	2.26 V
Max. charging voltage	2.9 V
Min. voltage	1.5 V
Max. charge current	130 A
Max. charge current	130 A
Operating temperature	-40°C to +55°C
Design life	25 years

In this section, the extension of the ETIS method to the multipoint ETIS is presented. The ETIS measurement was performed on the power optimized $LiMO_2$/ $Li_4Ti_5O_{12}$ with parameters presented in Table I. The test setup was custom made and it is based the high bandwidth Kepco High Power Bipolar Power Supply BOP 10-75MG (Figure 3, Figure 4). In order to improve the accuracy of temperature measurements, thermocouples were replaced with FLIR 8400SC thermal camera. This allows for much faster detection of battery surface temperature change caused by the thermal capacity of contact based temperature sensors (10).

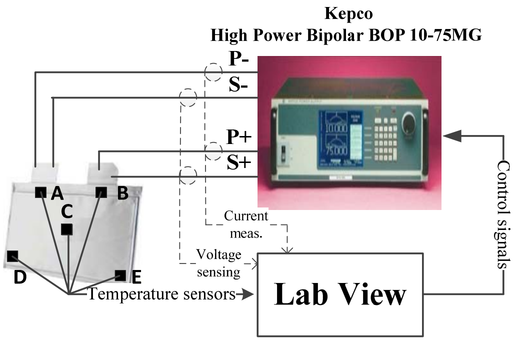

Figure 3 Schematic illustration of the test setup used for the multidimensional ETIS measurements.

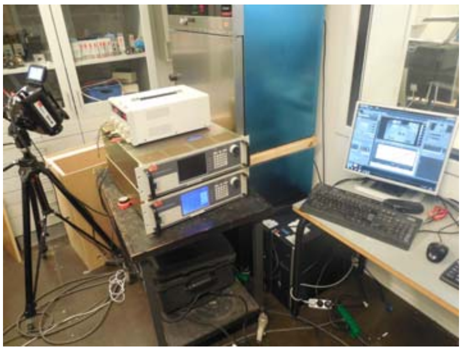

Figure 4 Laboratory test setup used for the multidimensional ETIS measurements.

The concept of the multipoint ETIS measurements allows for determining 'local' thermal capacities and thermal conductivities on the battery cell surface. These parameters can be later used for the parameterization of the 2D ETC based thermal models of battery cells like the one presented by Samba et al. in (11).

In the performed experiment, the temperature of five different spots on the li-ion battery surface was monitored during the frequency-based ETIS measurement (Figure 3). The localization of the spots was arbitrary chosen during initial measurements of the hot and cold spots of the battery cell during charging/discharging. The results for two battery spots are presented in Figure 5. It can be noticed that the temperature response to the sinusoidal heat excitation is also sinusoidal for all measured spots (Figure 6). Nevertheless, these sinusoidal temperature responses are different in terms of amplitude and phase depending on the spot location on the battery cell surface. In consequence, the thermal transfer function will be different depending on the spot location and it will result in different 'local' heat capacity and heat conductivity of the battery cell (Figure 7).

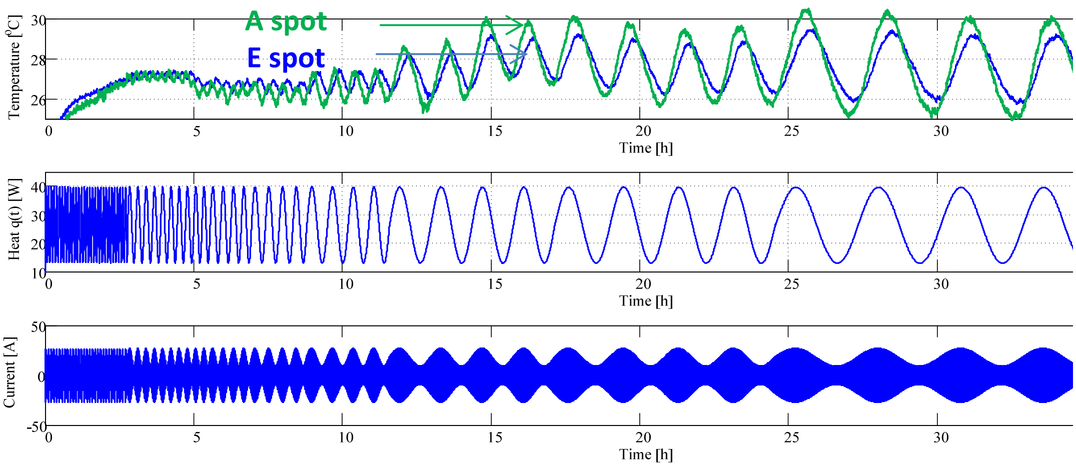

Figure 5 The obtained results from the frequency-based ETIS method on the $LiMO_2/Li_4Ti_5O_{12}$ battery cell. The temperature results are presented for two battery spots (A and E).

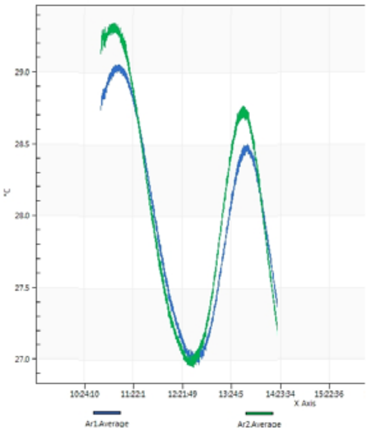

Figure 6 Zoomed part of the temperature response for spots A and E on the battery cell surface (difference in the amplitude and phase depending on the temperature measurement location in the battery cell).

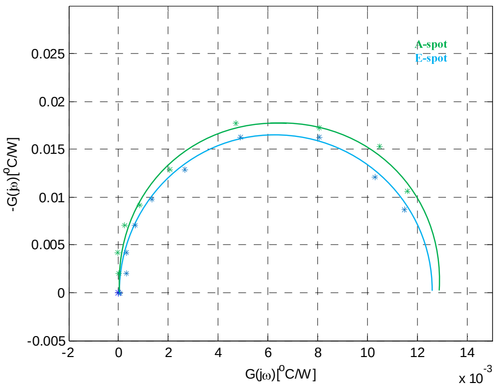

Figure 7 Comparison between A-spot and E-spot local thermal impedance for the $LiMO_2/Li_4Ti_5O_{12}$ battery cell.

Conclusions

The need for accurate and cost- and time-efficient to develop battery thermal models is increasing together with the increased power capability and compact design of the state of the art battery packs. The ETIS method has proven to be an efficient and non-destructive method, for the parametrization of the ETC-based thermal models of battery cells, that does not require any initial knowledge about battery cell's internal composition.

This paper presented initial measurements of the multipoint ETIS method that is an extension of the single point method. The provisional results allow for determining local thermal spectra of different battery cell spots. These findings can be further used for determining 'local' thermal capacities and heat conductivities and facilitate in the 2D ETC-based battery cell thermal model development.

The presented preliminary results needs to be further used for the parametrization of ETC-based 2D battery cell thermal model(s) in order to test the accuracy of the multipoint ETIS method.

Acknowledgments

Authors would like to acknowledge The Danish Council for Strategic Research for sponsoring the Advanced Lifetime Predictions of Battery Energy Storage (ALPBES) project.

References

1. P. M. Gomadam and R.E. White and W. Weidner, *J. Electrochem. Soc.*, **150**, A1339 (2003).
2. L. Song and W. Evans, Electrochemical-Thermal Model of Lithium Polymer Batteries, *J.Electrochem. Soc.*, **147**, 2086 (2000).

3. G. Guifang and L. Bo and C. Bo and Z. Shiqiong and X. Peng and C. Binggang, *J.Power Sources* **195**, 2393 (2010).
4. M. Hossein and K. S. Ahmad, *J. Power Sources* **115**, 131 (2003).
5. C. Forgez and D. V. Do and G. Freiedrich and M. Morcette and C. Delacourt, J. Power Sources; 195, 2961 (2010).
6. J.P. Schmidt and D. Manka and D. Klotz and E. Iver-Tiffe, *J. Power Sources*; **196**, 8140 (2011).
7. M. Fleckenstein and S. Fischer and O. Bohlen and B. Baker, *J. Power Sources*; **223**, 259 (2013).
8. E. Barsoukov and J.H. Jang and H. Lee, *J. Power Sources*, **109**, 313 (2002).
9. M. Swierczynski and D. Stroe and T. Stanciu and S.K. Kær, in *SDEWES 2015 Proceedings* (2015).
10. P. Keil and K. Rumpf and A. Jossen, in *EVS27 Proceedings* (2013).
11. A. Samba and N. Omar and H. Gualous and Y. Firouz and P.V den Bossche and J. V. Mierlo and T.I. Boubekeur, *Electrochemica Acta*, 117, 246 (2014).